

Homogenized material property prediction of carbon fiber composites using data-driven methods

Vipooshan Vipulanathan¹, Uditha Weerasinghe², Nisal Ariyasinghe^{2*},
Chinthaka Mallikarachchi² and Sumudu Herath²

¹Department of Computer Science and Engineering, Faculty of Engineering, University of Moratuwa, Bandaranayake Mawatha, Moratuwa, 10400, SRI LANKA.

²Department of Civil Engineering, Faculty of Engineering, University of Moratuwa, Bandaranayake Mawatha, Moratuwa, 10400, SRI LANKA.

Abstract

In this paper, several predictive models are tested for material property predictions of two-ply homogenized carbon fiber composites. The uncertainty of the constituent material properties yields uncertainties in the entries of the ABD stiffness matrix. These variations in the ABD stiffness entries are attempted to be captured using predictive models, namely, artificial neural networks and polynomial regression. Using Latin-Hypercube sampling technique, the constituent (fiber and resin) parameters are randomly sampled in the input space. For each entry in the input space, an ABD stiffness matrix is generated using a multiscale modeling technique and stored in the database as the output. Based on error estimates, the accuracy of predictions is evaluated using cross-validation on test folds. The non-zero entries in the A and D submatrices are observed to have very small prediction errors, whereas very small values appearing in B submatrix due to non-symmetric tow material properties are ignored. It is found that for the composite considered in this work, the linear regression model yields the highest accuracy whereas Neural network predictions are ranked second. This observation is justified as model training and testing were performed with less than a thousand data points, which is comparatively a low number for an artificial neural network model.

Keywords— Uncertainty quantification, Multiscale modeling, Computational homogenization, Machine learning, Neural networks, Polynomial regression, Predictive models

Introduction

Background

Utilizing fibre-based textile structures as the composite reinforcement results in making composite more tailorable and effective for applications where various types of loads are anticipated to support by the structure [1]. Also, this facilitates structures to be lightweight, adaptable, and durable. In light of this, fibre composite materials are widely employed in the aerospace industry.

The deployment of woven carbon fibre composites in deployable boom structures, such as the deployable antenna employed in the Mars Advanced Radar for Subsurface and Ionosphere Sounding (MARSIS) mission, is the main emphasis of this study. The full realisation of the potential behaviour of the structures following implementation is essential to the success of these missions [2]. But because to the challenges and limitations associated with establishing micro-gravity conditions, doing experimental research is challenging. Therefore, the main solution for understanding of the behaviour of these physical systems is through computer simulations.

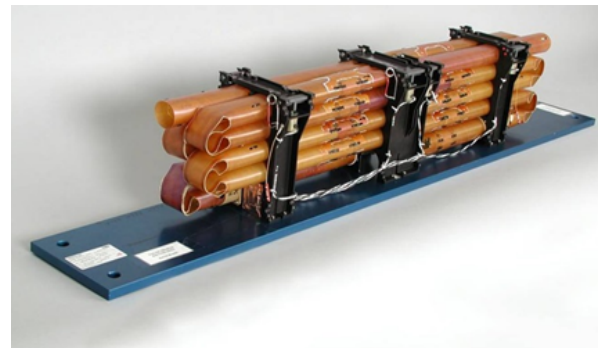


Figure 1: MARSIS deployable boom antenna

But both the complex geometry and non-linear behaviour of constituents of these composites make it more difficult to forecast the overall mechanical behaviour. The Multiscale modeling approach can be identified as a popular strategy to overcome this issue where several models at various scales are utilized simultaneously to describe the system. Typically, various models concentrate on various resolution scales.

The necessity of multiscale modeling typically results from inaccuracy, or the requirement of higher computational cost for the macroscale models and excess information provided by microscale models. Multiscale modeling can achieve good agreement

*Corresponding author: nariyasinghe@gmail.com

Received: March 16, 2023, Published: October 06, 2023

between efficiency and accuracy by merging those different scales simultaneously. Multiscale modelling requires identifying of the different scales accurately in terms of their geometry, material responses and underlined mechanics.

The mechanical or material inputs used for the macroscale analysis are based on ideal conditions. Therefore, uncertainties should be incorporated into these inputs in order to reflect the uncertainties that exist in the actual world. However, it costs an extensive amount of processing resources to represent both the macroscale and the microscale together. A predictive model would thus be highly beneficial in taking into account these uncertainties in the analysis.

Data-driven methods have paved their way into mechanical analysis, material design of systems and various other aspects related to continuum mechanics. A model is trained on a labelled dataset in supervised learning, a type of machine learning where the input data is linked to the matching output or target. Learning an input-output mapping will enable the model to generate precise predictions on brand-new data. In multiscale homogenization communities, these techniques are the tools of choice to mitigate the associated heavy computational cost and poor performance in nonlinear problems [3, 4]. These methods include Artificial Neural Networks (ANNs), Gaussian Process Regression (GPR), Polynomial Regression, Support Vector Machines (SVM), Graphical models, Sparse Kernel Machines, etc. [5]. Traditionally, ANNs are preferred in the absence of prior knowledge of the data or the process of data generation. Moreover, ANNs perform well in the presence of abundant data whereas techniques like GPR suffer from the curse of dimensionality at the presence of very large databases. In this paper, it is not intended to evaluate the suitability of available techniques, but to utilize widely used methods to predict the homogenized material properties of woven composites.

Related work

Investigations have been carried out to determine the effects of different parameters in the microscale to the mechanical properties in the macro scale in different research.

A tow is a material comprised of fibres and matrix that has a significant length and a relatively small cross-section. Plain woven composite is tailored by interlacing tows in warp and weft direction and impregnated with resin.

The research carried out by [6] investigates the effect of size and the relative positioning of the plies in the Representative Unit Cell (RUC) on the mechanical properties of a two-ply carbon fiber laminate.

The tow is homogenized to a transversely isotropic material and the tow path was idealized to a Cubic Bezier Spline curve during the modeling done using the Abaqus software. The boundary conditions were applied according to the Kirchhoff Love Plate theory and the ABD stiffness matrix was derived from the software. The outcomes of the analysis done by varying the RUC size highlight that the RUC size has no significant effect on the results except for Poisson's ratio. This provides a framework for the approach required for the multiscale model in this research.

A similar study was carried out by [7] using the Abaqus software to explore the response of the two-ply plain-woven carbon fiber composites with respect to different fiber volume fractions, traction coefficients, and fiber or matrix properties. The analyses done regarding the effects of fiber volume fractions exhibits the linear effect on the ABD stiffness matrix but also highlights that the Poisson's ratio remains immune to the variations in the fiber volume fractions. Surprisingly, the traction coefficients have negligible effects on the stiffness matrix except for the homogenized shear modulus. Nevertheless, it was determined that the mechanical characteristics of the composite were more influenced by the material properties. This provides the basis for the choice of introduction of uncertainties in the fibre and resin material properties in this research.

Multiscale modelling of woven carbon fibre composites

Theoretical review

Three sequential modelling scales may be used in models for both analytical and numerical studies to combine the requirements of different applications. Commonly used scales for textile composites are micro-mechanical, meso-mechanical, and macro-mechanical scales [8, 9]. Individual behaviour of resin and tows is emphasized in micromechanical scale taking into account their constituent properties, composition and the structure. Meso-mechanical modelling stage's fundamental focus is on understanding the mechanical behaviour of a Representative Unit Cell (RUC) considering tows as homogeneous structures. Macromechanical modelling stage simulates how the woven composite would behave under complex deformations.

Homogenization techniques combine two subsequent scales, through the selection of appropriate properties and distributions from acquisitions of the earlier scale.

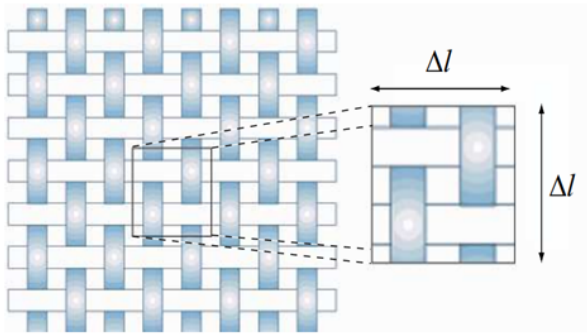


Figure 2: Representative Unit Cell (RUC) of size 2x2

Two-scale linear modelling of woven carbon fibre composites

In the micro-mechanical stage, idealized form of tows is three-dimensional continuums having transversely isotropic properties. Rules of mixtures, Halpin-Tsai semi-empirical relation [10] and a method proposed by [11] were used to estimate elastic constants of tows.

Fibre volume fraction of the considered laminate estimated by a weighting procedure [2] was 0.62. Assuming the entire fibre fraction of the model is concentrated in tows, $V_f = 0.62$ was used to characterize tows, averting possible voids in the laminate. Constituent properties were obtained from material specifications for HexPly 913 resin and T300-1k carbon fibres published by the manufacturer (Table 1). The material properties in the fibre and matrix are used to obtain the tow properties through rules of mixtures [7] and the homogenized properties of tows are presented in Table 2.

Table 1: Constituent properties (Source: Torayca. Technical Data Sheet No. CFA, T300 Data sheet. Toray Industries, Inc.)

Properties	Constituents	
	T300-1k fibre	HexPly 913 epoxy
Longitudinal stiffness, $E_1(N/mm^2)$	233,000	3,390
Transverse stiffness, $E_2(N/mm^2)$	23,100	3,390
Shear stiffness, $G_{12}(N/mm^2)$	8,963	1,210
Poisson's ratio, $\nu_{12}(N/mm^2)$	0.2	0.41
Density, $\rho(kg/m^3)$	1,760	1,230
Areal weight of fabric/film, $W(g/m^2)$	98	30

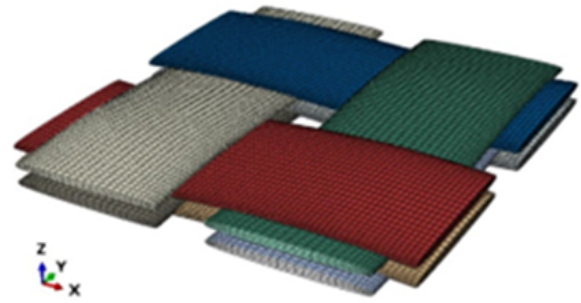


Figure 3: Dry fibre RUC

Table 2: Tow properties

Tow Properties	Value
Longitudinal Young's modulus, $E_1(N/mm^2)$	145,748
Transverse stiffness, $E_2 = E_3(N/mm^2)$	10,427
Shear stiffness, $G_{12} = G_{13}(N/mm^2)$	3,378
In-plane Shear stiffness, $G_{23}(N/mm^2)$	3,498
Poisson's ratio, $\nu_{12} = \nu_{23}$	0.28
Poisson's ratio, ν_{23}	0.49

In the mesomechanical stage, 2x2 RUC was selected in agreement with a previously done study on size effect [6]. Geometrical parameters which were selected congruent with the micrographs of the considered laminate [2] are presented in Table 3.

Table 3: Geometrical parameters

Parameters	Values
Wavelength, L (mm)	2.664
Maximum tow thickness, $h(mm)$	0.059
Tow cross sectional area, $A(mm^2)$	0.052

RUC's tow geometry was created using the readily available finite element pre-processor TexGen and exported into Abaqus/Standard finite element software package for simulations. For the examined laminate, a cubic Bezier spline towpath was selected with an in-phase tow arrangement commensurate with previous studies [12]

The tow cross section was approximated as a power ellipse shape of $n=0.5$ (where n is an input parameter of Texgen software) which is matching with micrographs [2]. Eight-node linear brick elements with reduced integration (C3D8R) were used for tows (Figure 3)

Inter-connection between contact surfaces was modelled with surface based cohesive constraints to incorporate inter-tow slipping behaviour. ‘Surface-to-surface’ discretization was used to minimize the large penetration of slave nodes. Linear elastic traction separation was used to define cohesive behaviour with traction stiffness values of 253,722 MPa/mm for normal mode and 90,561 MPa/mm for shearing and tearing modes.

Boundary nodes were connected to multiple reference points created at the mid-plane of RUC using ‘MPC beam’ constraints. A Dummy node was created per each pair of reference points at two boundaries and related using ‘Equation constraints’ to apply deformations and to extract data. Periodic boundary conditions were defined as stated in [2] to represent the continuum nature of the composite.

Homogenized material response

ABD matrix constitutes the relationship between kinematic variables (mid-plane strains and curvatures) and static variables (mid-plane force resultants and moment resultants of the laminate).

$$\begin{Bmatrix} N_x \\ N_y \\ N_{xy} \\ M_x \\ M_y \\ M_{xy} \end{Bmatrix} = \begin{bmatrix} A_{11} & A_{12} & A_{16} & B_{11} & B_{12} & B_{16} \\ A_{12} & A_{22} & A_{26} & B_{12} & B_{22} & B_{26} \\ A_{16} & A_{26} & A_{66} & B_{16} & B_{26} & B_{66} \\ B_{11} & B_{12} & B_{16} & D_{11} & D_{12} & D_{16} \\ B_{12} & B_{22} & B_{26} & D_{12} & D_{22} & D_{26} \\ B_{16} & B_{26} & B_{66} & D_{16} & D_{26} & D_{66} \end{bmatrix} \begin{Bmatrix} \epsilon_x \\ \epsilon_y \\ \epsilon_{xy} \\ \kappa_x \\ \kappa_y \\ \kappa_{xy} \end{Bmatrix} \quad (1)$$

where N is the force per unit length, M is the moment per unit length, ϵ is the mid-plane strain, κ is the mid-plane curvature, $[A]$ sub-matrix denotes the extensional stiffness matrix, $[B]$ sub-matrix denotes the extension-bending coupling matrix, and $[D]$ sub-matrix denotes the bending stiffness matrix.

Six separate analyses were performed for each unit deformation (i.e., $\epsilon_x = 1$, and $\epsilon_y = \epsilon_{xy} = \kappa_x = \kappa_y = \kappa_{xy} = 0$) by introducing strains and curvatures to the RUC through dummy nodes and associated displacements, rotations of the reference nodes and forces and moments of the dummy nodes were extracted. MATLAB code was used to construct the ABD matrix following the principle of virtual work.

In order to calculate entities in the ABD matrix, equalised the external work done by the given unit deformation (as unit strain) and the internal work done by the boundary nodes by multiplying forces from the dummy nodes which are applied to the boundary nodes (since those are connected by equation constraints) and the deformations of boundary nodes.

For the first deformation mode, were applied unit axial strain in the x direction. Hence, by the principle of virtual work,

$$\epsilon_x^2 A_{11} \Delta l_x l_y = \sum_{BN} (F_x u + F_y v + F_z w + M_x \theta_x + M_y \theta_y + M_z \theta_z) \quad (2)$$

For linear analysis, all the used strain values were in unit magnitude ($\epsilon_x = 1$). The calculation was extended for all entities of the ABD matrix using a MATLAB code and the obtained matrix is presented in Eq. 3.

$$ABD = \begin{bmatrix} 8493 & 2195 & 0 & 0 & 0 & 1 \\ 2195 & 8493 & 0 & 0 & 0 & 1 \\ 0 & 0 & 370 & 0 & 0 & 0 \\ 0 & 0 & 0 & 36.5 & 4.7 & 0 \\ 0 & 0 & 0 & 4.7 & 36.5 & 0 \\ 2 & 0 & 0 & 0 & 0 & 1.8 \end{bmatrix} \quad (3)$$

Data generation

For model training and testing the required data points are generated as follows. The weighted average tow properties given in Table 2 are better understood by the constituent properties in Table 1. Hence, the Latin hypercube quasi-random sampling of the input space is performed by considering a $\pm 5\%$ variation of all constituent material parameters of each tow. For instance, a single data point in the input space of the database is a 8×2 matrix where 8 refers to the eight tows in the RUC of the composite and 2 refers to the two constituents; fibre and resin. Thus, the applied variation will generate new material properties, like in Table 1, and in turn change the tow properties in Table 2. The variation factor for fibre (c_f) and resin (c_r) is always distinct and further, c_f of each tow takes different values to maintain the randomness of sampling. A single data point in the input space takes the form;

The output for a single data point will be the ABD stiffness matrix, which is generated after performing multiscale modelling as described in the previous sections of this paper. For model training, entries in the B sub-matrix is not considered despite its small values due to the non-symmetric material properties of tows. Herein, the entries in A and D sub-matrices are considered for model training, testing and prediction phases of the data-driven models. In this work a

Table 4: Data points in the input space

Cf	0.998, 1.040, 1.031, 1.008, 0.966, 1.021, 0.959, 0.981
Cr	0.977, 0.997, 1.030, 1.047, 1.010, 0.966, 0.956, 1.022

total of 967 data points are generated at a cost of 40 minutes per data point.

Data-driven prediction of ABD parameters

Review of data-driven techniques

In this work, the implementation of machine learning algorithms has allowed for the prediction of ABD parameters. In recent years, data-driven models have gained increasing popularity. When integrated with machine learning approaches, these models seem to be more potent, and are able to predict without having any prior understanding of the system and capable to attain higher accuracy. For this study, we use a several well-known machine learning algorithms and statistical methods for comparison purposes.

Correlation

In a regression model, multicollinearity occurs when two or more independent variables are highly correlated with one another. As seen from the heatmap in Figure 4, there are no two or more predictors that are highly linearly related, so multicollinearity was not an issue in this case, thus lower variable redundancies.

Polynomial regression

Regression analysis is a statistical technique for determining the relationship between various variables. The use of regression analysis in machine learning for prediction is currently a hot topic. The regression analysis is used to find out how the dependent variable is changing when one independent variable is changing, and other independent variables are remained unchanged. Mostly it is used to determine the average value of the dependent variable for fixed independent variable values [13].

Linear regression (LR) is a statistical technique that is used to model the relationship between the dependent variable (also called the response) Y and one or more independent variables (also called explanatory) X . The regression function represents the function Y , and it can be expressed by the equation:

$$Y = \beta_0 + \beta_1 X + \epsilon \tag{4}$$

Where: Y is the dependent variable (response). X is the independent variable (explanatory). β_0 is the y -intercept (the value of Y when X is 0). β_1 is the slope of the line (represents the change in Y for a unit change in X). ϵ represents the error term or

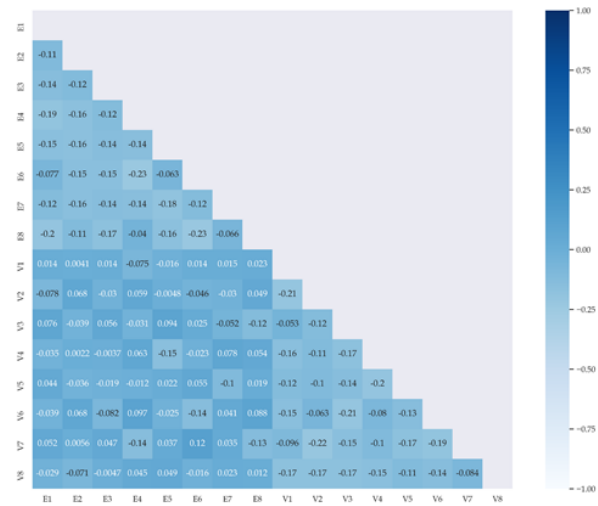


Figure 4: Correlation matrix of variables

residual (the difference between the observed Y and the predicted Y).

The input dataset contains y and x values, which are used by linear regression to create a predictive model, particularly for tasks like forecasting. The trained model is expected to predict the value of Y for a new x value. Linear regression is a widely used technique for understanding and predicting relationships between variables in various fields of study. [13].

Neural networks

Artificial Neural Network (ANN) is a technology which is developed to emulate a biological neural network based on the studies on the human brain and nervous system. The processing elements of the human brain which are the neurons are connected to each other. These neurons are arranged in a layer where the output from one layer is given as input to other layers. The neurons receive the input signal from other neurons or external stimuli and process them using a transfer or activation function. There are many variants of ANN models. Amongst them, the multi-layer perceptron (MLP) is the most influential for a study considered in this paper [14].

The MLP model has several layers of nodes where the first layer acts as an input layer which receives external information, and the last layer acts as the output layer which produces the final output for the problem. There will be one or more intermediate layers between the input layer and the output layer. These layers are called as hidden layers. There will be acyclic arcs connecting the nodes of lower layer to a higher layer [14].

Repeated cross validation

The most recommended cross-validation method for machine learning models of both classification and regression is repeated K-fold. The repeated K-fold algorithm’s main process involves repeatedly shuffling and randomly sampling the data set, and it produces a robust model by covering the most training and testing processes. Two parameters are required for this cross-validation procedure to function accordingly in assessing the performance of a predictive model. The given dataset (i.e. the total data volume including training and testing data set) will be divided into K folds according to the first argument, K, which represents an integer value (or subsets). The model is trained on the K-1 subsets of the K folds, and the performance of the model will be tested on the remaining subset. (Repeated K-fold Cross Validation in R Programming - GeeksforGeeks, 2022)

NRMSE

The Normalized Root Mean Squared Error (NRMSE) is an error estimate, that enables users to compute the error between estimated and observed values using various normalizing techniques. The comparison of predictions over models with various scales is made easier by using a normalized RMSE. NRMSE takes the form,

$$NRMSE = \sqrt{\frac{1}{n} \sum_{i=1}^n (y_i - \hat{y})^2 / \bar{y}} \quad (5)$$

where

- y_i = Output form the data (training/testing)
- \hat{y} = Output form the model (training/testing)
- $\bar{y} = \frac{1}{n} \sum_{i=1}^n y_i$

Results and discussion

Model training using polynomial fitting

As there are few parameters in the linear regression model, it was chosen with default parameters. Scatter plot for actual vs prediction of linear regression is shown in Figure 5. The best features were chosen using GridSearchCV which belongs to the model selection package of the sklearn library (sklearn.model_selection.GridSearchCV,2022). Fitting the estimator (model) to the given training set will allow to iterate through specified hyper-parameters. For better performance, all sixteen features in the input space were chosen.

As observed in Table 5 and Table 6, $D_{2,2}$ and $D_{1,1}$ received low NRMSE scores, while $A_{1,2}$ and $A_{2,6}$ received high NRMSE score in comparison to other

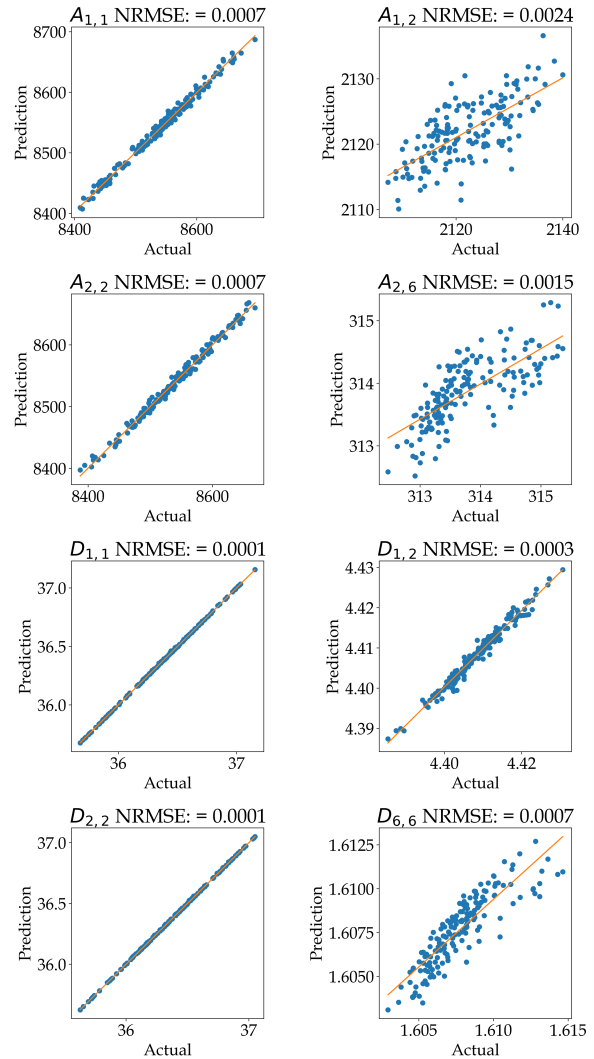


Figure 5: Scatter plot for actual vs prediction of linear regression

dependent variables. The variations between scores in the train and test for same variables and difference between each train score and corresponding test score do not vary significantly. This indicates that the model has not over-fitted.

Model fitting using ANNs

The resulted architecture ANN model is shown in Figure 6. It consists of one input layer, two hidden layers and one output layer. More hidden layers were also explored, but the model’s performance did not improve yet the complexity of the architecture. As a result, the proposed simple architecture was chosen since it produced superior error estimates.

As seen in the Table 8 and Table 9, compared to the scores of linear regression, $D_{6,6}$, $A_{2,6}$ and $A_{1,2}$ only received low NRMSE scores and unlike linear regression, $D_{1,2}$ received a higher NRMSE score compared to other dependent variables, although it is

Table 5: NRMSE score of the train dataset (repeated cross validation)

Fold	A11	A12	A22	A66	D11	D12	D22	D66
0	7.0E-04	2.5E-03	6.9E-04	1.5E-03	9.0E-05	2.9E-04	8.7E-05	6.6E-04
1	6.9E-04	2.6E-03	7.1E-04	1.5E-03	9.1E-05	2.9E-04	8.5E-05	6.4E-04
2	6.9E-04	2.5E-03	7.0E-04	1.5E-03	8.7E-05	2.8E-04	8.7E-05	6.7E-04
3	7.1E-04	2.5E-03	7.1E-04	1.5E-03	8.9E-05	2.9E-04	8.5E-05	6.9E-04
4	7.1E-04	2.6E-03	7.1E-04	1.5E-03	9.0E-05	2.9E-04	8.5E-05	6.7E-04
5	7.1E-04	2.6E-03	7.1E-04	1.5E-03	8.4E-05	3.0E-04	8.4E-05	6.5E-04
6	6.9E-04	2.5E-03	7.0E-04	1.5E-03	9.0E-05	2.8E-04	8.7E-05	6.6E-04
7	6.9E-04	2.6E-03	7.1E-04	1.5E-03	9.0E-05	2.9E-04	8.6E-05	6.8E-04
8	7.0E-04	2.5E-03	7.0E-04	1.5E-03	9.1E-05	2.9E-04	8.6E-05	6.8E-04
9	7.0E-04	2.5E-03	7.0E-04	1.5E-03	9.1E-05	2.9E-04	8.6E-05	6.6E-04

Table 6: NRMSE score of the test dataset (repeated cross validation)

Fold	A11	A12	A22	A66	D11	D12	D22	D66
0	7.1E-04	2.8E-03	7.7E-04	1.6E-03	9.0E-05	3.1E-04	8.2E-05	7.1E-04
1	7.7E-04	2.5E-03	7.0E-04	1.6E-03	8.4E-05	2.9E-04	9.3E-05	7.8E-04
2	7.5E-04	2.6E-03	7.3E-04	1.6E-03	1.0E-04	3.1E-04	8.4E-05	6.7E-04
3	6.8E-04	2.6E-03	7.2E-04	1.4E-03	9.4E-05	2.8E-04	9.2E-05	6.1E-04
4	6.7E-04	2.5E-03	6.9E-04	1.5E-03	8.8E-05	2.9E-04	9.1E-05	6.8E-04
5	6.7E-04	2.5E-03	6.9E-04	1.5E-03	1.1E-04	2.6E-04	9.5E-05	7.4E-04
6	7.5E-04	2.6E-03	7.2E-04	1.4E-03	8.8E-05	3.2E-04	8.3E-05	7.0E-04
7	7.4E-04	2.6E-03	7.1E-04	1.5E-03	8.8E-05	2.8E-04	8.8E-05	6.3E-04
8	7.1E-04	2.7E-03	7.5E-04	1.6E-03	8.6E-05	3.1E-04	8.8E-05	6.2E-04
9	7.2E-04	2.7E-03	7.4E-04	1.6E-03	8.6E-05	3.0E-04	8.7E-05	7.1E-04

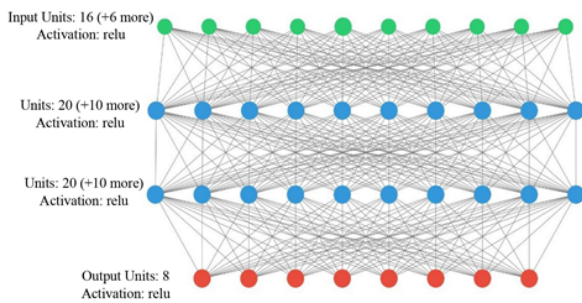


Figure 6: Model architecture of ANN

Table 7: ANN model summary

Layer	Type	Number of neurons
0	Input	16
1	Hidden	20
2	Hidden	20
3	Output	8

still lower than the score obtained in linear regression. The variations between scores in the train and test for same variable are high compared to results of linear regression. This reveals that linear regression provides consistent results for each K-split.

Result comparison

The dataset was scaled using a standard scaler since it is recommended for the better performance of data-driven methods. Without scaling features, the same algorithms may be biased towards the features with higher magnitudes. It is also mentioned that prediction values were descaled to actual scale before calculating NRMSE values [4].

According to the overall mean shown in Table 10 and Table 11, the results of both train and particularly test data sets revealed that the linear regression (0.00084) performed better than ANN (0.00110). The test results for $A_{1,1}$, $A_{2,2}$, $D_{1,1}$, $D_{1,2}$, and $D_{2,2}$ in linear regression shows significant improvement compared to those for ANNs. Conversely, for $A_{1,2}$, $A_{6,6}$ and $D_{6,6}$, the test results of ANN are marginally superior to those of linear regression. These findings demonstrate that linear regression (LR) outperforms Artificial Neural Networks (ANNs) for $A_{1,1}$, $A_{2,2}$, $D_{1,1}$, $D_{1,2}$, and $D_{2,2}$. The superiority of LR can be

Table 8: NRMSE score of the train dataset (repeated cross validation)

Fold	A11	A12	A22	A66	D11	D12	D22	D66
0	8.8E-04	2.2E-03	9.0E-04	1.3E-03	7.9E-04	3.4E-04	7.0E-04	4.4E-04
1	8.6E-04	2.2E-03	8.9E-04	1.3E-03	7.5E-04	3.0E-04	7.4E-04	4.4E-04
2	8.8E-04	2.2E-03	9.4E-04	1.2E-03	8.5E-04	3.2E-04	7.9E-04	4.2E-04
3	9.6E-04	2.3E-03	8.2E-04	1.2E-03	8.4E-04	3.4E-04	6.3E-04	4.3E-04
4	9.2E-04	2.3E-03	1.0E-03	1.1E-03	7.7E-04	3.5E-04	7.7E-04	4.6E-04
5	9.5E-04	2.2E-03	9.1E-04	1.3E-03	7.9E-04	3.3E-04	8.0E-04	4.4E-04
6	9.3E-04	2.3E-03	1.0E-03	1.1E-03	7.3E-04	3.6E-04	7.5E-04	4.3E-04
7	8.6E-04	2.3E-03	9.3E-04	1.2E-03	7.1E-04	3.0E-04	6.6E-04	4.5E-04
8	8.7E-04	2.2E-03	8.8E-04	1.2E-03	6.8E-04	3.3E-04	6.9E-04	4.5E-04
9	9.7E-04	2.2E-03	9.9E-04	1.1E-03	8.2E-04	3.6E-04	7.6E-04	4.5E-04

Table 9: NRMSE score of the test dataset (repeated cross validation)

Fold	A11	A12	A22	A66	D11	D12	D22	D66
0	8.9E-04	2.8E-03	9.4E-04	1.5E-03	7.8E-04	3.4E-04	7.1E-04	5.1E-04
1	1.0E-03	2.5E-03	1.1E-03	1.5E-03	8.3E-04	3.7E-04	8.4E-04	5.4E-04
2	1.1E-03	2.7E-03	1.0E-03	1.6E-03	1.1E-03	4.3E-04	9.0E-04	4.9E-04
3	1.1E-03	2.5E-03	9.8E-04	1.3E-03	1.1E-03	4.2E-04	7.7E-04	5.3E-04
4	1.0E-03	2.5E-03	9.6E-04	1.4E-03	8.7E-04	4.3E-04	9.8E-04	5.1E-04
5	9.7E-04	2.5E-03	9.8E-04	1.4E-03	7.6E-04	4.0E-04	9.0E-04	5.5E-04
6	1.1E-03	2.6E-03	1.1E-03	1.3E-03	8.6E-04	4.3E-04	8.4E-04	6.5E-04
7	9.8E-04	2.6E-03	9.8E-04	1.5E-03	7.0E-04	3.5E-04	7.5E-04	4.9E-04
8	9.6E-04	2.7E-03	1.1E-03	1.5E-03	7.8E-04	4.1E-04	8.2E-04	5.1E-04
9	1.0E-03	2.6E-03	1.1E-03	1.4E-03	8.8E-04	3.9E-04	7.9E-04	4.7E-04

Table 10: Overall Train mean NRMSE score for Each target

	A11	A12	A22	A66	D11	D12	D22	D66	Mean
ANN	9.1E-04	2.2E-03	9.3E-04	1.2E-03	7.7E-04	3.3E-04	7.3E-04	4.4E-04	9.4E-04
LR	7.0E-04	2.5E-03	7.0E-04	1.5E-03	8.9E-05	2.9E-04	8.6E-05	6.7E-04	8.2E-04

Table 11: Overall Test mean NRMSE score for Each target

	A11	A12	A22	A66	D11	D12	D22	D66	Mean
ANN	1.0E-03	2.6E-03	1.0E-03	1.4E-03	8.6E-04	4.0E-04	8.3E-04	5.2E-04	1.1E-03
LR	7.2E-04	2.6E-03	7.2E-04	1.5E-03	9.2E-05	3.0E-04	8.8E-05	6.9E-04	8.4E-04

attributed to its suitability for datasets with linear relationships, its simplicity, and better generalization on smaller datasets. Additionally, LR's interpretability provides valuable insights, while ANNs may lack transparency due to their complexity. Overall, linear regression dominates here with mean test score 0.00084 (< 0.00110).

Other well-known machine learning models were also tested including tree-based models such as Support Vector Regression, Random Forrest and XGBoost. However, they did not outperform linear or ANN models and hence are not presented in this paper. In both model training and testing stages, linear regression outperformed the ANN models. According to

the overall mean linear regression performed better than ANNs.

Conclusions

In this paper, the importance of constructing predictive models to predict the homogenized response of carbon fibre composites is explored. The uncertainties of material parameters at the microscale are propagated to the macroscale via multiscale modelling and subsequently used to train the predictive models. In this work, both linear regression and ANNs are explored in the presence of a relatively smaller

dataset. Overall, the linear regression model predicted the material parameter variations better than the ANNs. Though this observation is unexpected in a general context (due to the proven performance of ANNs) the smaller number of data points (967) in the database has led to the superior performance of linear regression models over ANNs. It is concluded that the ABD material parameters are well captured by linear regression models, where NRMSE values of predictions are well below 0.00084.

References

- [1] Navid Shekarchizadeh, Mohammad Mahdi Abedi, and Reza Jafari Nedoushan. "Prediction of elastic behavior of plain weft-knitted composites". In: *Journal of Reinforced Plastics and Composites* 35.22 (2016), pp. 1613–1622.
- [2] HM Mallikarachchi. "Thin-walled composite deployable booms with tape-spring hinges". PhD thesis. University of Cambridge, 2011.
- [3] Sumudu Herath. "Multiscale modelling and material design of woven textiles using Gaussian processes". In: *Acta Mechanica* 233.1 (2022), pp. 317–341.
- [4] Sumudu Herath, Xiao Xiao, and Fehmi Cirak. "Computational modeling and data-driven homogenization of knitted membranes". In: *International Journal for Numerical Methods in Engineering* 123.3 (2022), pp. 683–704.
- [5] Christopher M Bishop and Nasser M Nasrabadi. *Pattern recognition and machine learning*. Vol. 4. 4. Springer, 2006.
- [6] Milindu Jayasekara et al. "Size Effect and Fibre Arrangement on Meso-Mechanical Modelling of Woven Fibre Composites". In: *2021 Moratuwa Engineering Research Conference (MERCon)*. IEEE. 2021, pp. 124–129.
- [7] Sumudu Herath, Milindu Jayasekara, and Chinthaka Mallikarachchi. "Parametric Study on the Homogenized Response of Woven Carbon Fibre Composites". In: *2020 Moratuwa Engineering Research Conference (MERCon)*. IEEE. 2020, pp. 36–41.
- [8] Ramin Bostanabad et al. "Uncertainty quantification in multiscale simulation of woven fiber composites". In: *Computer Methods in Applied Mechanics and Engineering* 338 (2018), pp. 506–532.
- [9] Wei Tao et al. "Uncertainty quantification of mechanical properties for three-dimensional orthogonal woven composites. Part II: Multi-scale simulation". In: *Composite Structures* 235 (2020), p. 111764.
- [10] Robert M Jones. *Mechanics of composite materials*. CRC press, 1998.
- [11] Shunjun Song et al. "Compression response of 2D braided textile composites: single cell and multiple cell micromechanics based strength predictions". In: *Journal of composite materials* 42.23 (2008), pp. 2461–2482.
- [12] Saranja Nadarajah, Milindu Jayasekara, and Chinthaka Mallikarachchi. "Nonlinear bending response of two-ply plain woven carbon fibre composites". In: *2019 Moratuwa Engineering Research Conference (MERCon)*. IEEE. 2019, pp. 147–151.
- [13] Petrovski Aleksandar, Petrusseva Silvana, and Zileska P Valentina. "Multiple linear regression model for predicting bidding price". In: *Technics Technologies Education Management* 10.3 (2015), pp. 386–393.
- [14] Guoqiang Zhang, B Eddy Patuwo, and Michael Y Hu. "Forecasting with artificial neural networks: The state of the art". In: *International journal of forecasting* 14.1 (1998), pp. 35–62.